Title
Does the trabecular bone score reflect the structure of trabecular bone?

Author
Lee, Tae Je

Publication Date
2015

Peer reviewed|Thesis/dissertation

Does the trabecular bone score reflect the structure of trabecular bone?

by

Tae Je Lee

THESIS

Submitted in partial satisfaction of the requirements for the degree of

MASTER OF SCIENCE

in

Biomedical Imaging

in the

GRADUATE DIVISION

of the

[redacted]

Acknowledgement

First and foremost, I would like to thank Dr. Thomas Lang for giving me this wonderful opportunity to work on this extremely enjoyable and educational research project. His patience and guidance through the entire length of my work has been invaluable. His encouragement kept me optimistic throughout my project and I cannot have wished for a better advisor and mentor.

Dr. Klaus Engelke's previous work with the simulated x-rays was crucial in obtaining images and masks we needed. I thank him and Dr. Oleg Museyko for finding the time to help me with my research, and sharing their data, masks, calibration parameters.

I would also like to thank Dr. Xiaojuan Li, Dr. Galateia Kazakia and, Dr. Sharmila Majumdar for their support and advice as members of my Thesis Committee.

I would also like to thank Dr. Julio Carballido-Gamio for his help with my Matlab codes.

In addition, I would like to thank all of my classmates in the MSBI program for making classes and assignments fun and also for being great friends.

I thank Dr. Martin Alastair, and Dr. David Saloner for providing us with a great program, and attending to all our administrative, educational and personal needs.

Lastly, I would like to thank my parents for their continued support, and my siblings for their words of encouragement in all of my endeavors.

Does the trabecular bone score reflect the structure of trabecular bone?

(Tae Je Lee)

Abstract

Introduction

Trabecular bone score (TBS) was proposed as a method to indirectly assess the vertebral microarchitecture from Dual X-ray Absorptiometry (DXA) images, which are have a projectional geometry that does not reflect 3D structure. In this study, we evaluated the extent to which TBS is affected by the variable angulation of the vertebra in the body and the presence of aortic calcifications that overly the vertebra.

Methods

All programming was done on Matlab. The CT data was provided by Dr Sundeep Khosla's group at the Mayo Clinic from their study of age-related bone loss and fracture. Partial vertebral masks, calibration data, and coordinate transforms, were provided by Professor Engelke's group. Calcified aorta was removed from each slice manually. We computed the TBS of a pure trabecular bone region in a standardized ("bone fixed") vertebral coordinate system as a gold standard. This was compared via linear regression to the TBS of the entire vertebra in the bone fixed coordinate system and then to the entire vertebra in the native scanner coordinate system. Both comparisons were done with and without the aortic calcium removed.

Results

There was a modest but significant correlation observed between the TBS of pure trabecular bone region and the TBS of the image set in bone-fixed coordinate with the calcified aorta

removed. The correlation degraded slightly when calcified aorta was added back in, and degraded heavily when the images were rotated back to their original scanner coordinates. There was a correlation observed between rotation angle and the TBSs between the original and rotated image sets.

Conclusion

There was a significant reduction of correlation between TBS of pure trabecular bone region and the TBS calculated from native images in the scanner coordinate system with aortic calcification. As the angle of rotation increased, greater deviation was noticed between the TBS of the original and the rotated image. We conclude that the poor correlation between the pure trabecular bone and the native TBS raises significant questions about the clinical utility of this technique.

Table of Contents

List of Tables:

List of Figures:

List of Figures:

List of Figures:

Background

Osteoporosis is a disease marked by low bone mass, and deterioration of bone structure that increases the risk of fracture. [1] It is often called the "silent disease", because before resulting in a fracture, often from a minor fall or similar activity, it progresses asymptomatically. Osteoporosis is estimated to affect 200 million women worldwide, and in women over 45 years of age, it accounts for more days spent in hospital than many other diseases, including diabetes, myocardial infarction and breast cancer. [2] The disability due to osteoporosis is comparable or greater than that disability introduced by variety of other chronic diseases, such as rheumatoid arthritis, asthma, and high blood pressure. [9] U.S. Department of Health & Human Services report that for the population at risk for osteoporotic fractures, most strongly established for post-menopausal women with BMD scores in the osteoporosis range with pre-existing fractures but well established for patients of all age, medications, such as bipohsphonates, denosumab, raloxifene, and teriparatide, will significantly decrease fracture risk. [10] Therefore, ability to screen for and accurately predict osteoporosis in the at-risk population is highly sought after.

Dual X-ray Absorptiometry (DXA) is X-ray imaging method currently used to diagnose osteoporosis. It generates a 2D projected image of the bone, from which the areal bone mineral density (aBMD), is calculated. The X-rays that travel through the tissue are absorbed differently depending on the type of tissue they travel through. The bone tissue, due to its high mineral content, creates strong contrast in X-ray images. Lower aBMD is correlated with higher fracture risk, and is currently the gold standard used by the World Health Organization in diagnosis of osteoporosis. [3]

There are a number of problems with relying solely on DXA for diagnosis of osteoporosis. Notably, it does not utilize any evaluation of the 3D bone architecture, which contributes strongly to the bone strength and other biomechanical properties. [4] Many patients with fracture do not necessarily have low aBMD. [5] However, it is impractical with current technology and availability to generate a 3D CT image for hip or the vertebrae that accurately portrays the patient's trabecular bone microarchitecture. This has motivated proposed techniques to evaluate the trabecular bone microarchitecture from the widely available 2D DXA images.

Trabecular bone score (TBS) was proposed as a way to indirectly assess the vertebral microarchitecture from DXA images. [6] It is a grey-level texture measurement that uses a variogram of the 2D DXA image. It is based on the fact that a healthy patient has well-structured trabecular bone at the vertebral level, but an osteoporotic patient has an altered trabecular bone structure. This means healthy patient's trabecular structure is dense, with high connectivity, high trabecular number, and small spaces between trabeculae, and osteoporotic patient's trabecular structure is porous, with low connectivity, low trabecular number, and wide spaces between trabeculae. [6] On a 2D projected image, the healthy patient's trabecular bone would be spatially heterogeneous, having a high number of pixel value variations, with the overall amplitudes of these variations being small, whereas for an osteoporotic patient's trabecular bone, it would have a low number of pixel value variations, with the overall amplitudes of these variations being large. This is illustrated in figure 1.

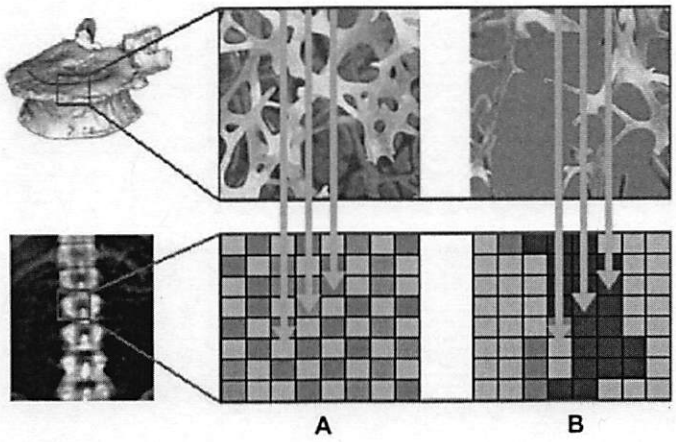

Figure 1. Illustration of 3D trabecular bone architecture and its corresponding 2D DXA image for healthy (A) and osteoporotic (B) patients. [Hans, D. et. al]

It has been shown that the TBS, calculated from DXA images of human cadaver lumbar vertebrae, is significantly correlated with the 3D microarchitecture of the trabecular bone. [6,7] Re-analyses of DXA images from population studies have shown that low TBS values are associated with increased vertebral fracture risk even when low aBMD is taken into account. However, there are a number of factors that can disrupt the correspondence between TBS and the trabecular microarchitecture, such as aortic calcification, variable rotation of vertebrae, and image noise. The goal of our study is to gain insight in how heterogeneity of the vertebra in areal images of the entire vertebra reflects the heterogeneity of pure trabecular bone, and we will achieve this by simulating key clinical sources of error in TBS.

Materials and Methods

We used 333 series of CT images of the lumbar spine in subjects from a study of age-related changes in bone using CT, done by Professor Klaus Engelke's group at the University of Erlangen. [8] Only the first 52 series were used for the axis of rotation calculations, due to their computation intensiveness. 3D CT data was used to be able to manipulate the data in the 3D space, as well as to be able to project the data to a planar 2D image, mimicking what the corresponding DXA image would be. We first calibrated the scans from Hounsfield Units to equivalent hydroxyapatite concentration in g/cm3, and used a custom thresholding algorithm in conjunction with the partial segmentations mapped out in the previous study to segment the posterior regions of the vertebrae.

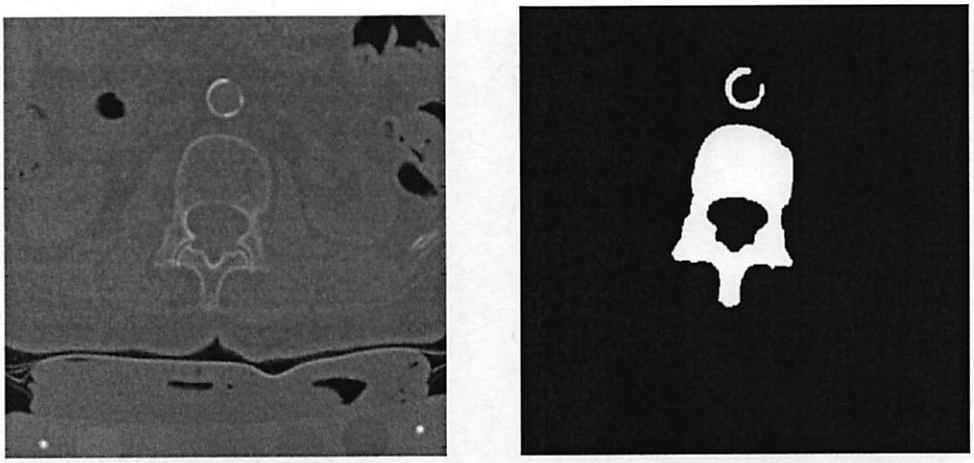

Figure 2. An example slice from the CT dataset, and its segmented vertebral mask.

Within the laboratory (scanner) coordinate system, we projected the calibrated 3D CT image and segmentation of the entire vertebra onto the coronal image plane and the coronal planar mask of

the desired vertebrae. The projected CT image and the planar mask can be combined to generate a BMD map of the segmented vertebrae.

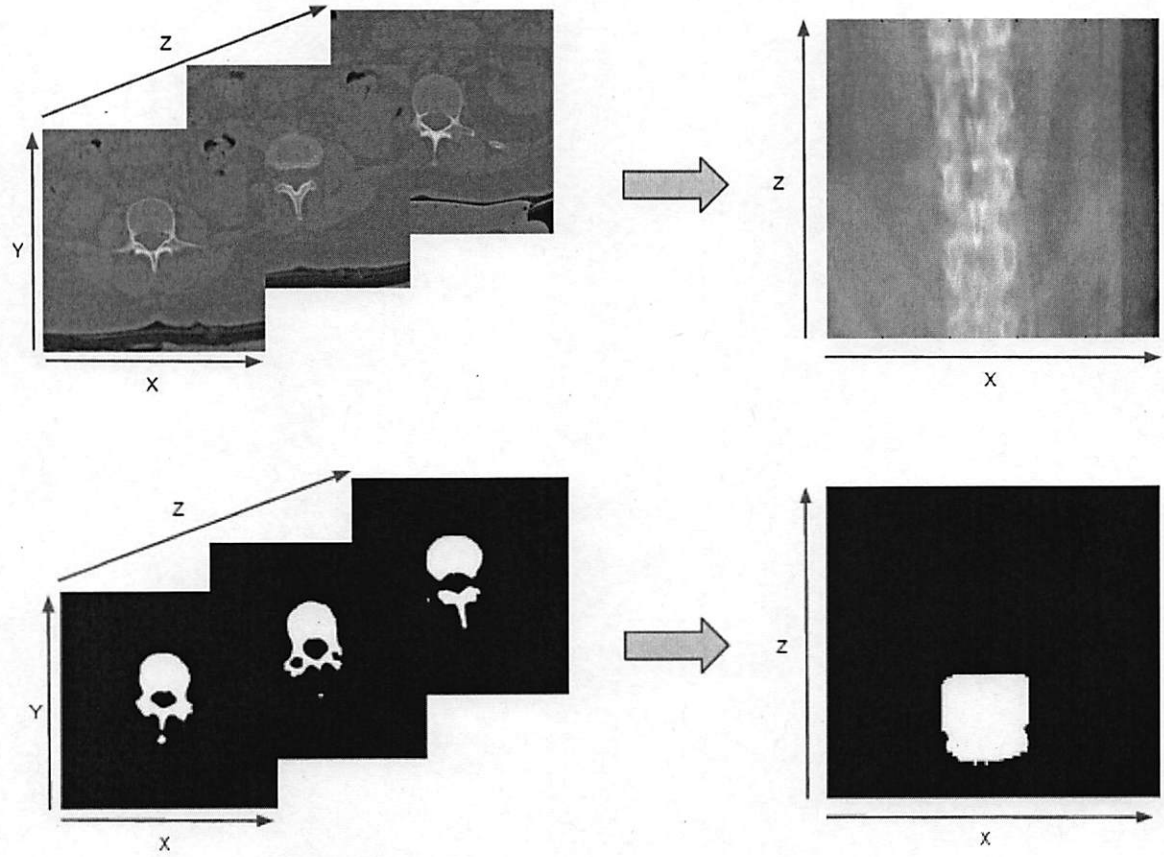

Figure 3. Example slices are projected in y-direction, resulting in a coronal image of the spine.

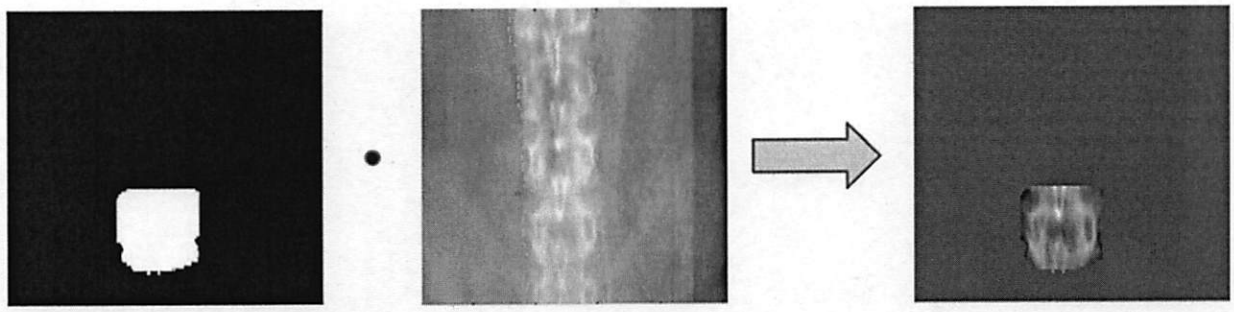

Figure 4. Coronal planar mask and its corresponding coronal projected image are combined to generate a coronal planar image of the segmented vertebrae. Each vertebrae is highlighted in yellow.

We then calculate the Trabecular Bone Score (TBS), using the following algorithm:

$$V(k) = \left\langle \left[P\left(\vec{M}_0 + k * \vec{u_\theta}\right) - P\left(\vec{M}_0\right) \right]^2 \right\rangle$$

where

k	the unit distance (varying from 0 to 10, in steps of 1 pixel)
$V(k)$	the experimental variogram function, representing the grey level variations in function of the distance k;
$\vec{M}_0$	the initial point in the 2D projection image P
θ	the angle defining a direction from the horizontal line passing through $\vec{M}_0$
$\vec{u_\theta}$	the unit vector in the θ direction

A random point and an angle is chosen in the generated BMD map, and intensity differences squared are recorded for each pixel distances, from one pixel to ten.

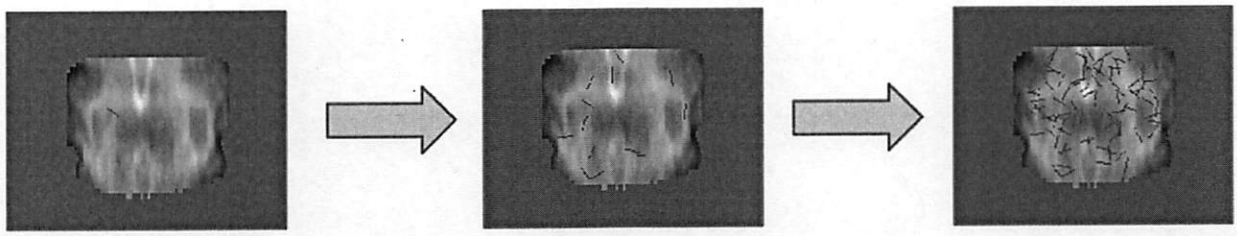

Figure 5. Illustration of the random line selection process on the generated BMD map.

10,000 points and angles were picked for each BMD map. TBS was defined as the slope of the line of linear fit when the average differences squared were plotted for pixel distances 1 to 10 on a log-log graph.

The archived coordinate transformation files were used to rotate the vertebrae and their segmented masks into a coordinate system with the z-axis perpendicular to the endplates, or the

bone-fixed coordinate system. New projections were generated for the images in the bone-fixed coordinate system, and their TBS were calculated. The coordinate transform files included a point of origin, which is selected to be at the center of the vertebrae of interest, and three vectors that marked the new axial, sagittal, and coronal axes. Angle of rotation around each axis was found, and applied in correct order on the dataset. Resulting dataset in fractional coordinates were interpolated using a custom written 3d linear interpolation.

Then, the calcified aorta were removed from the generated masks. These new sets of masks containing no calcified aorta were projected on to a coronal image, and then rotated accordingly. From these two new projected images, we calculated their trabecular bone scores.

Finally, using the existing segmentations of the trabecular bone volume, provided by Klaus Engelke's group, we created a new set of masks containing only trabecular bone. After it was coordinate rotated to the bone-fixed coordinate system, its TBS calculated. This group of TBS is from pure trabecular bone, in the bone-fixed coordinates, and containing no calcified aorta, which are the sources of error we are investigating. This was used as the gold standard of the TBS, and the correlations between the gold standard and other set of TBS each containing an error source of interest were examined.

Figure 6. Illustration of the process of removing calcified aorta from the generated mask.

The TBS of the pure trabecular bone and the TBS of the entire vertebra in the bone-fixed coordinate system with aortic calcifications should be have strongly correlated. We evaluated how that correlation degrades when the images were subjected to these sources of error. The correlation between the TBS of the pure trabecular bone to the TBS of the image in the scanner frame will bring insight on the effect of variable vertebral orientation on TBS, while the correlation between the TBS of the pure trabecular bone to the TBS of the image in the bone-fixed frame with calcified aortas retained will bring insight on the effect of presence of such artifacts on TBS. Finally, the correlation between the TBS of the pure trabecular bone to the TBS of the image in the scanner frame with osteophytes and aortic calcification will represent how strong the TBS correlation will be under most realistic conditions.

All Matlab codes were custom coded. The CT images, partial masks, coordinate transforms and calibrations were provided by Klaus Engelke's group. They are from an older study involving osteoporotic women. [8] Each CT data set, from a patient, was centered on the vertebrae of the

lumbar region. Each data set was read in, with its corresponding 3-dimensional trabecular region mask of the L1 vertebrae. L-2 vertebrae were chosen if the CT data of the L-1 vertebrae was not of high quality.

$$Correl(X,Y) = \frac{\sum (x-\bar{x})(y-\bar{y})}{\sqrt{\sum (x-\bar{x})^2 \sum (y-\bar{y})^2}}$$

Figure 7. Correlation Coefficient Function used to calculate the Pearson's R-value.

To determine the rotation angle effects and the TBS correlation degradation, rotation angle around each axis was plotted against the percentage TBS difference between the images in the scanner frame and the images in the bone-fixed frame were plotted and compared.

Results

	Scan. Co. w/ CA	*Bone. Co. w/ CA*	*GS*	*Scan. Co. w/o CA*	*Bone. Co. w/o CA*
Scanner Coord. With CA	1				
Bone-fixed Coord. With CA	0.708146382	1			
Gold Standard	0.48804562	0.687735154	1		
Scanner Coord. Without CA	0.939011015	0.719694867	0.496200599	1	
Bone-fixed Coord. Without CA	0.682958507	0.934303233	0.690462409	0.704648143	1

Table 1. Correlation coefficient (Pearson's R-value) between TBS calculated from various image datasets under different manipulations.

Table 1 shows the correlation coefficients between each of the data sets and the gold standard. Figures 8, 9, 10, and 11 show the correlation between the TBS calculated from the gold standard and the TBS calculated from the images in scanner coordinates retaining the calcified aorta, images in bone-fixed coordinates retaining the calcified aorta, images in the scanner coordinates with the calcified aorta removed, and images in the one-fixed coordinates with the calcified aorta removed, respectively.

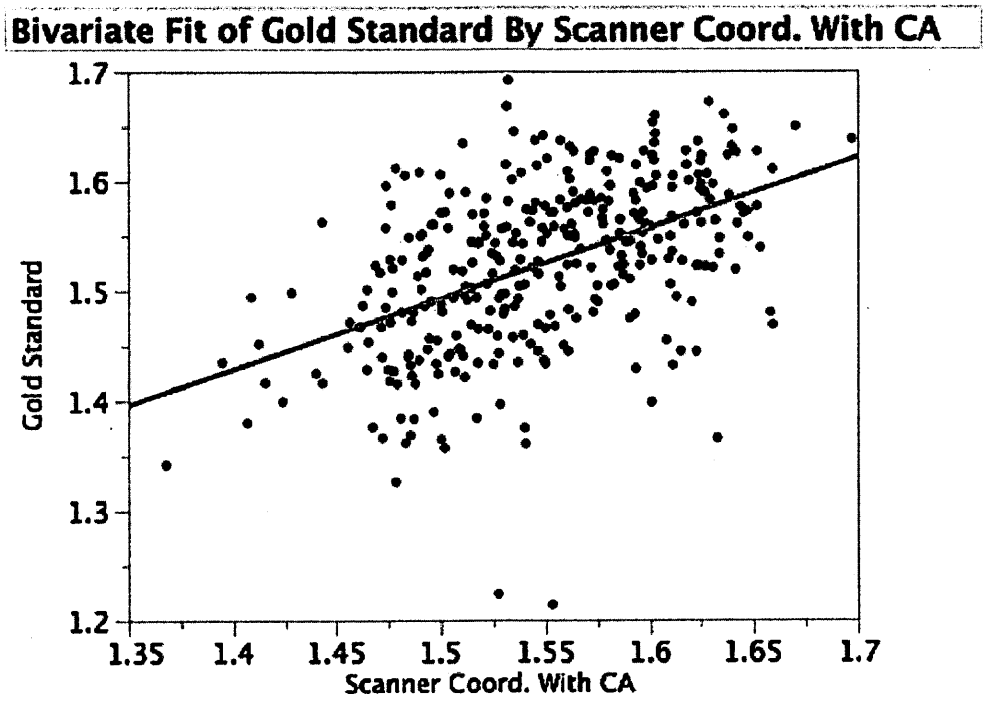

Figure 8. Bivariate plot of the Trabecular Bone Score calculated from the projected dataset in the scanner coordinate system with Calcified Aorta retained vs. the Trabecular Bone Score calculated from the Gold Standard. R-squared value is 0.238189.

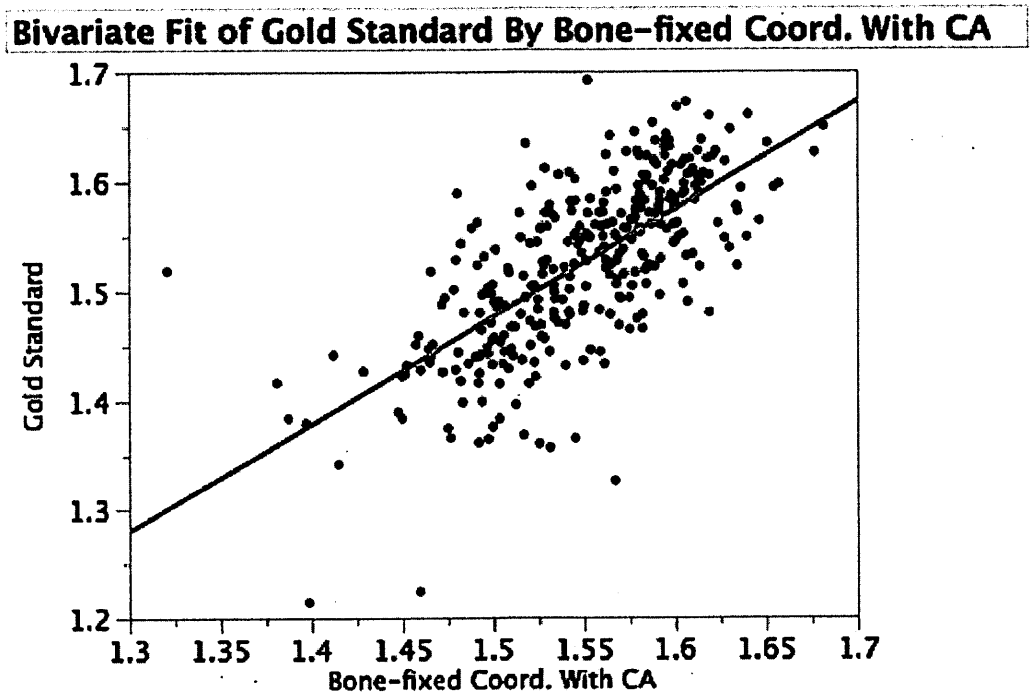

Figure 9. Bivariate plot of the Trabecular Bone Score calculated from the projected dataset in the bone fixed coordinate system with Calcified Aorta retained vs. the Trabecular Bone Score calculated from the Gold Standard. R-squared value is 0.47298.

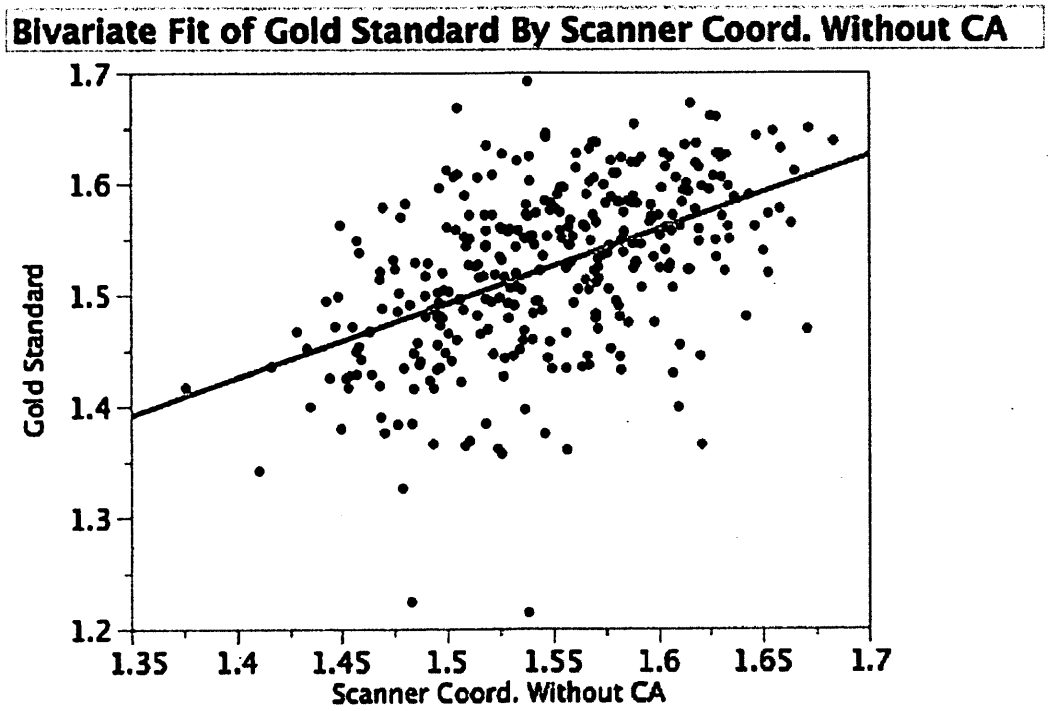

Figure 10. Bivariate plot of the Trabecular Bone Score calculated from the projected dataset in the scanner coordinate system with Calcified Aorta removed vs. the Trabecular Bone Score calculated from the Gold Standard. R-squared value is 0.246215.

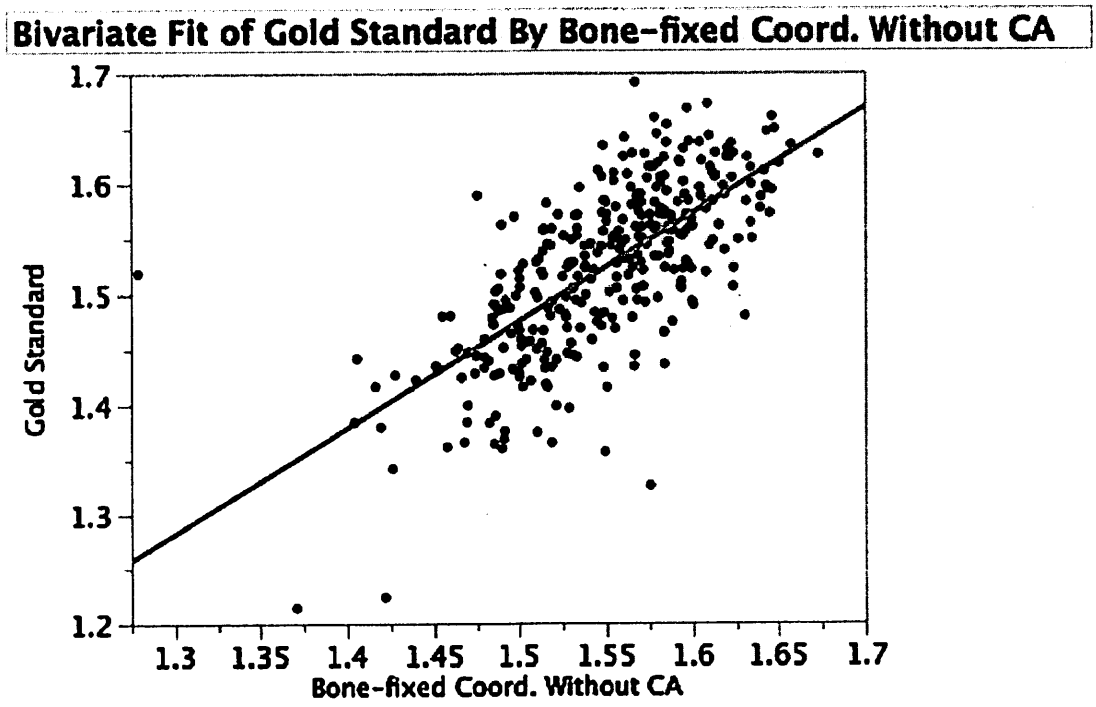

Figure 11. Bivariate plot of the Trabecular Bone Score calculated from the projected dataset in the bone fixed coordinate system with Calcified Aorta removed vs. the Trabecular Bone Score calculated from the Gold Standard. R-squared value is 0.476738.

Figures 12 and 13 show the correlation between the TBSs of image sets in the scanner coordinate system and the bone-fixed coordinate system, with and without aortic calcification, respectively. Figures 14 and 15 show the correlation between the TBSs of image sets with and without aortic calcification, in the scanner and bone-fixed coordinate systems, respectively.

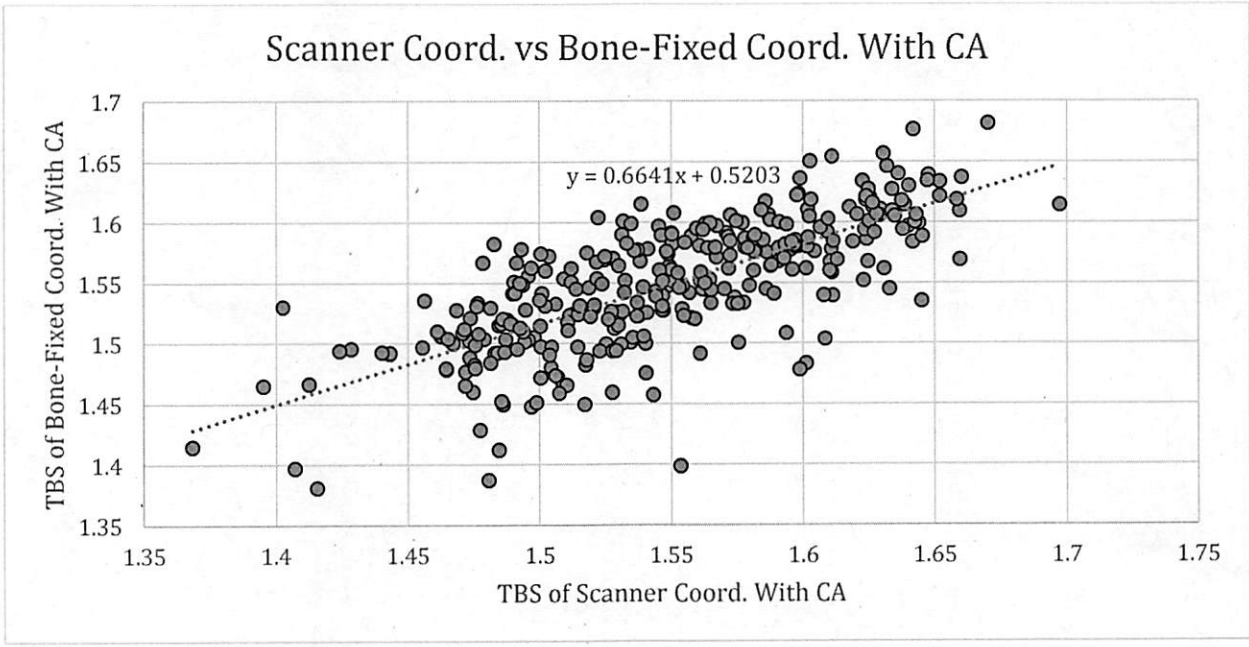

Figure 12. Bivariate plot of the Trabecular Bone Score calculated from the projected dataset in the scanner fixed coordinate system with Calcified Aorta retained vs. Trabecular Bone Score calculated from the projected dataset in the bone fixed coordinate system with Calcified Aorta retained. R-squared value is 0.5282.

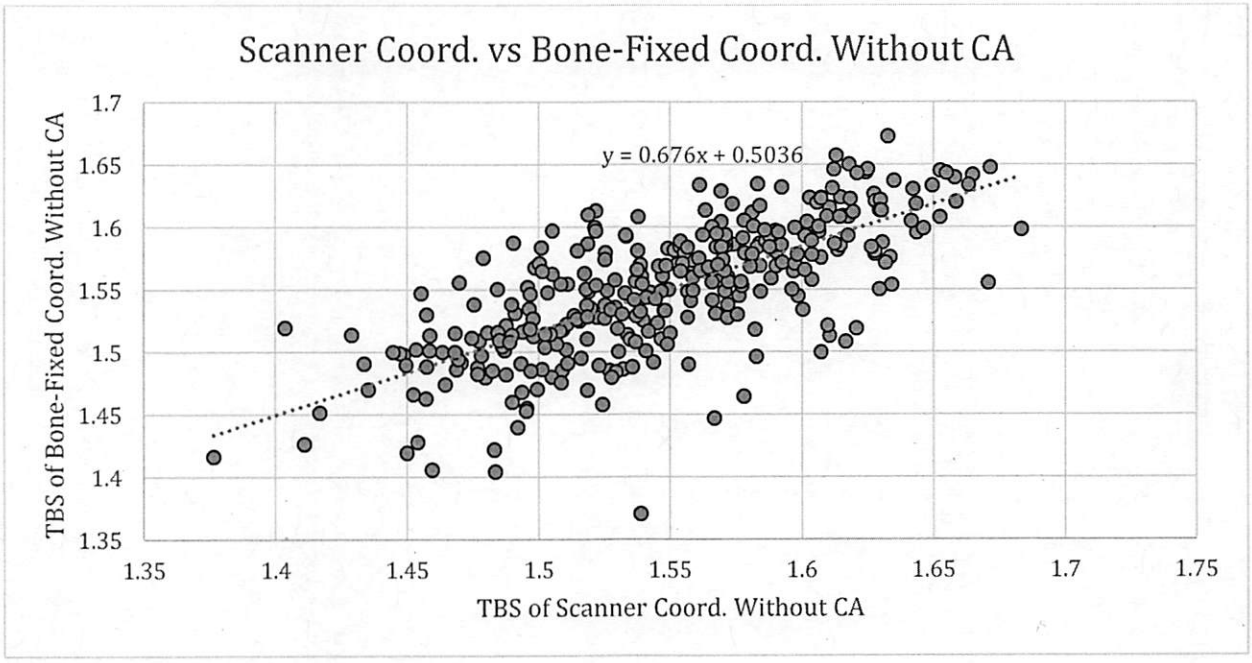

Figure 13. Bivariate plot of the Trabecular Bone Score calculated from the projected dataset in the scanner fixed coordinate system with Calcified Aorta removed vs. Trabecular Bone Score calculated from the projected dataset in the bone fixed coordinate system with Calcified Aorta removed. R-squared value is 0.4858.

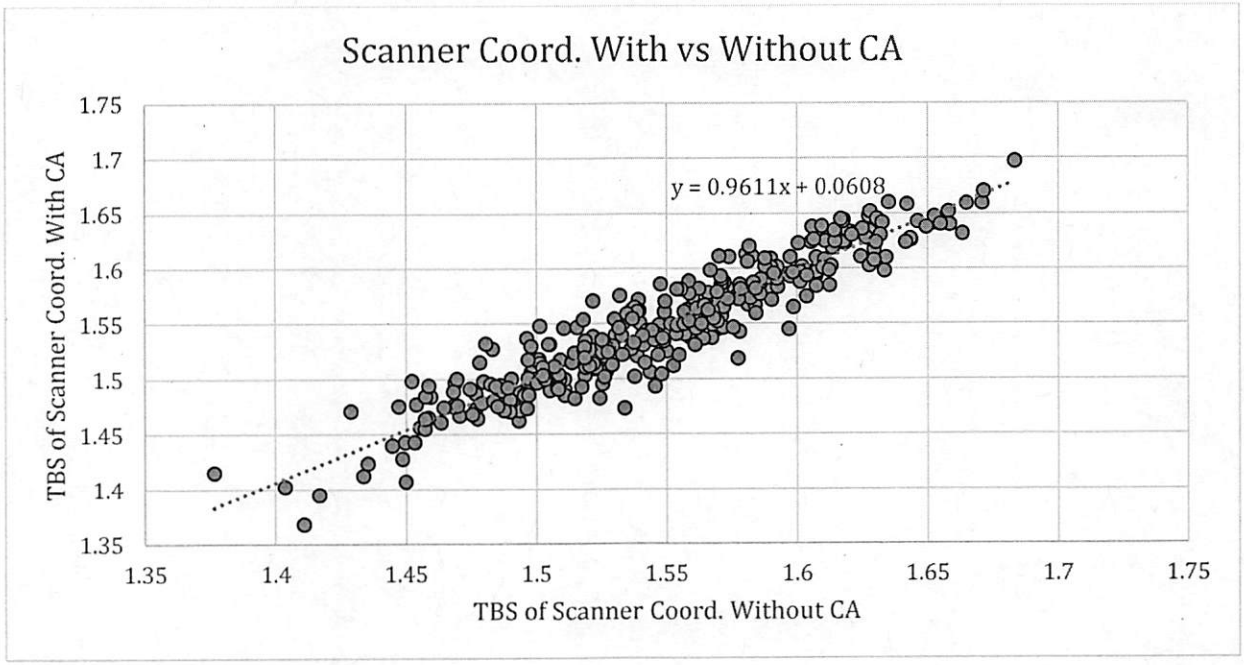

Figure 14. Bivariate plot of the Trabecular Bone Score calculated from the projected dataset in the scanner fixed coordinate system with Calcified Aorta retained vs. Trabecular Bone Score calculated from the projected dataset in the scanner fixed coordinate system with Calcified Aorta removed. R-squared value is 0.8834.

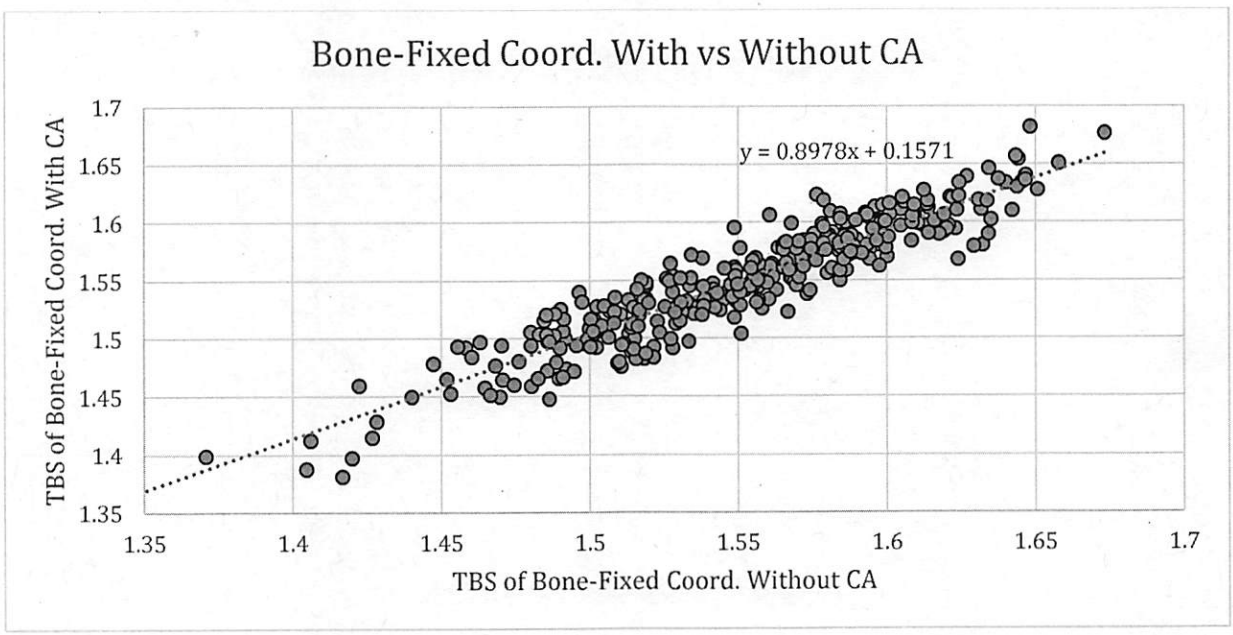

Figure 15. Bivariate plot of the Trabecular Bone Score calculated from the projected dataset in the bone fixed coordinate system with Calcified Aorta retained vs. Trabecular Bone Score calculated from the projected dataset in the bone fixed coordinate system with Calcified Aorta removed. R-squared value is 0.8685.

	Rotation (no CA)	Rotation (CA)	CA (Bone-Fixed)	CA (Scanner)
Average %difference between TBS	0.472926164	0.621219635	0.111807536	0.352524853

Table 2. Average percentage difference from rotation, with and without Calcified Aorta removed, and from removing Calcified Aorta, in the bone fixed coordinate system and in the scanner system.

Table 2 shows the average percentage difference between the TBSs due to rotation, with and without calcified aorta, and due to presence of calcified aorta, in bone-fixed and scanner coordinate systems. Table 3 shows the correlation coefficients between TBS difference between scanner and bone-fixed images, matched against angles of rotation around the sagittal, coronal, and axial axis.

	Sag. Angle	*Cor. Angle*	*Axi. Angle*	*TBS diff.*
Sag. Angle	1			
Cor. Angle	0.139462	1		
Axi. Angle	0.341955	0.24045	1	
TBS difference	0.242893	-0.07068	0.279739	1

Table 3. Correlation coefficient (Pearson's R-value) between TBS difference in percentage between the coordinate systems with Calcified Aorta removed and the rotation angle around the three axis.

Figures 16, 17, and 18 show the correlation between TBS differences due to rotation, and the angle of rotation around the sagittal, coronal, and axial axis, respectively. Because rotation wasn't applied independently of each axis, but rather directly taken from how the patient was oriented naturally in the scanner, we see large amount of scatter in the data.

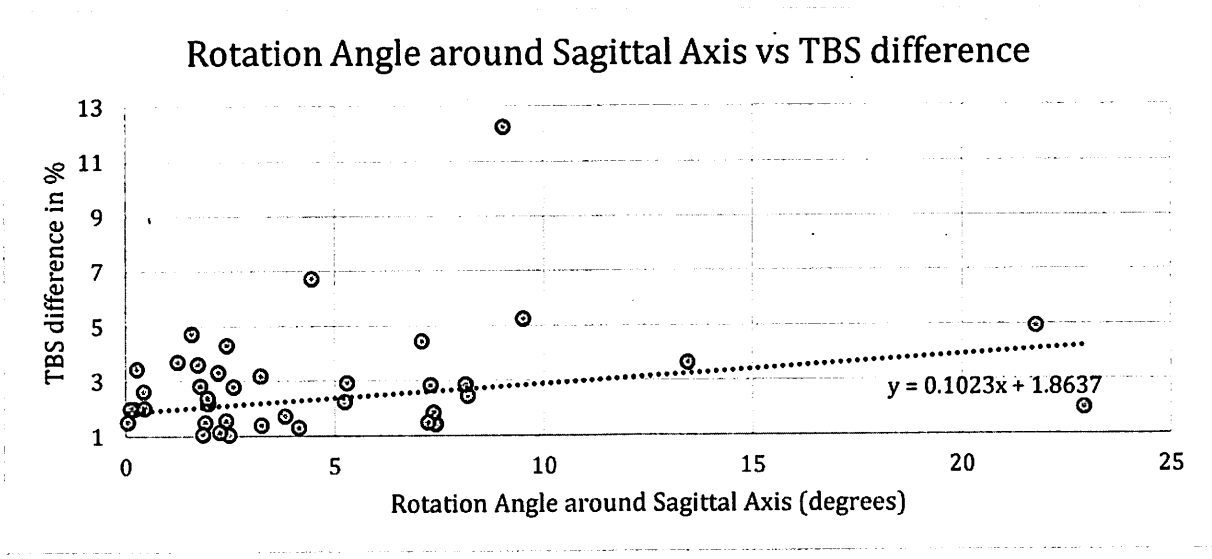

Figure 16. Bivariate plot of the rotation angle around the sagittal axis in the image vs. Trabecular Bone Score difference in percentage between the projected dataset in the bone fixed coordinate system and the scanner coordinate system all with Calcified Aorta removed.

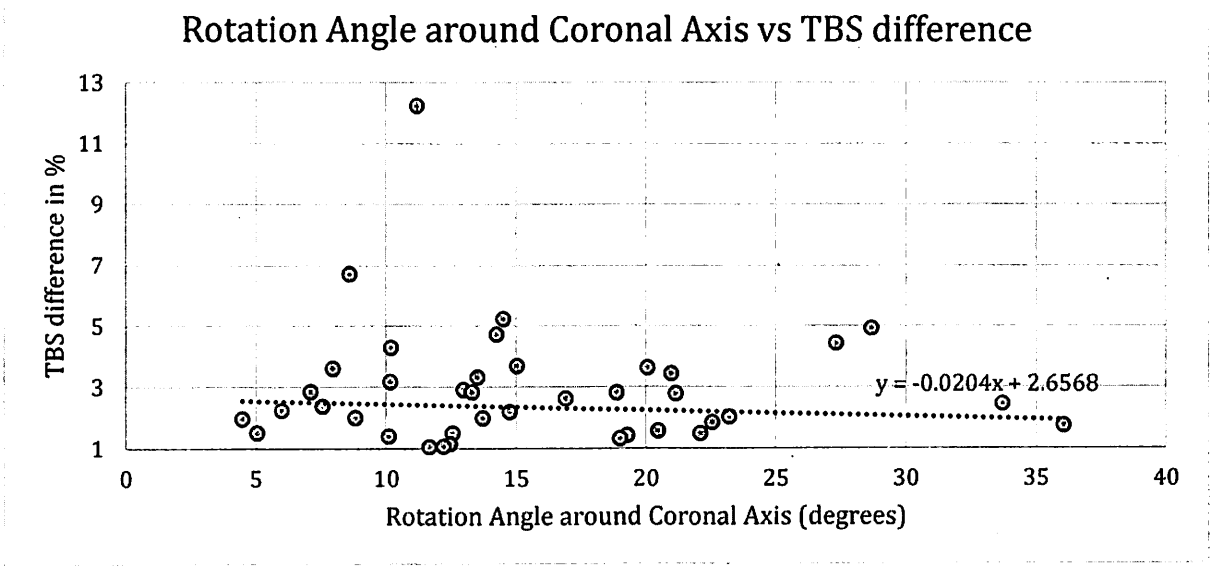

Figure 17. Bivariate plot of the rotation angle around the coronal axis in the image vs. Trabecular Bone Score difference in percentage between the projected dataset in the bone fixed coordinate system and the scanner coordinate system all with Calcified Aorta removed.

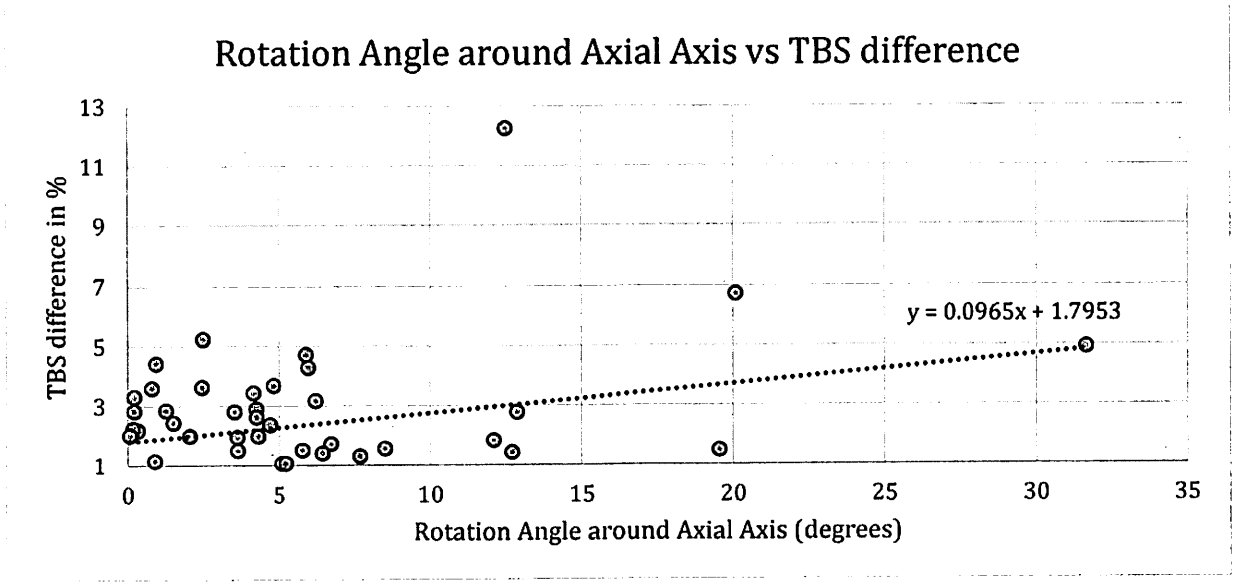

Figure 18. Bivariate plot of the rotation angle around the axial axis in the image vs. Trabecular Bone Score difference in percentage between the projected dataset in the bone fixed coordinate system and the scanner coordinate system all with Calcified Aorta removed.

When we examine angle of rotation around the sagittal axis while keeping the angles of rotation around other axis to zero, we see that as the angle of rotation gets larger, TBS tends to deviate more.

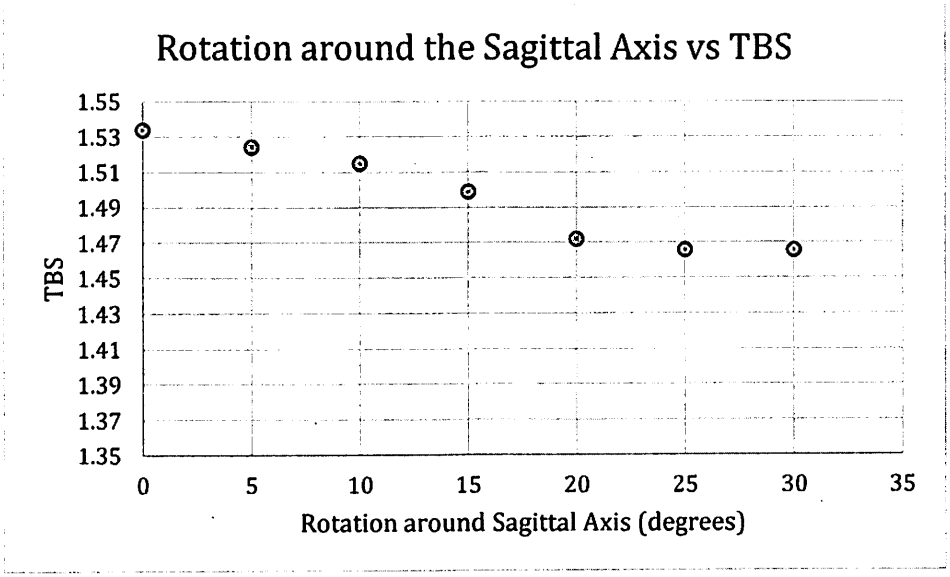

Figure 19. Plot of the angle of the rotation around the sagittal axis against the TBS.

Discussion

In this work, we explored the how might the correlation between the TBS calculated from the 2D projected image and the actual TBS calculated from the pure trabecular region degrade as the data was rotated and in the presence of calcified aorta. As hypothesized, the TBS calculated from the image in the bone-fixed frame with calcified aorta removed had the best correlation with the TBS calculated from the gold standard. When the calcified aorta were included back in the images, the correlation degraded from 0.690 to 0.688, while returning the images from bone-fixed coordinates to the scanner coordinates degraded the correlations from 0.690 to 0.496. When both source of errors were subjected to the images, correlation degraded down to 0.488. The variable angle resulting from spine scoliosis and patients not aligned perfectly to the scanner had a stronger degrading effect on the TBS correlation than the presence of calcified aorta. We furthered explored the angle effect by comparing the percentage differences in TBS stemming from rotation with the angles in the three rotation axis. We found weak correlations in the rotation angles around the sagittal and axial axis and the percentage differences, 0.242 and 0.279 respectively, and no correlation in the rotation angle around the coronal axis, at -0.070. Because the TBS was calculated from a coronal planar image, we found it reasonable that rotating around the coronal axis would have little to no impact on the TBS, while the rotations around the other two axis did have an impact. Because rotations around each axis weren't considered on their own, we observed high scatter. To control for this effect, we kept the rotation around the coronal and axial axis to zero, while incrementally increased the rotation around sagittal axis, as shown in Figure last. There, we observed a decreasing trend in TBS as the rotation angle became larger, but this varying angle experiment was done only for one data series due to its computation intensiveness, and to fully explore this effect, the experiment needs to be done with more data.

Conclusion

By manipulating 3D CT data of various patients, we were able to control which sources of errors were included in the generated projected images. Their TBS were calculated and were compared. Our results show that both variable angle of the scan and the presence of calcified aorta has a degrading effect on the correlation of the image TBS to the gold standard, with variable angle having a much greater impact than the presence of calcified aorta. Overall, we find using trabecular bone score as an unreliable technique in clinical diagnosis of osteoporosis, unless the sources of error mentioned in the paper can be controlled for.

References

[1] American Academy of Orthopaedic Surgeons, "Osteoporosis and bone health," AAOS Now, (2009), http://www.aaos.org/news/aaosnow/may09/clinical8.asp

[2] International Osteoporosis Foundation, "Osteoporosis Facts and Statistics," http://www.iofbonehealth.org/facts-and-statistics/index.html

[3] Roberts, B. J. et. al., "Comparison of hip fracture risk prediction by femoral aBMD to experimentally measured factor of risk," Bone, Volume 46, no.3, 742-6. (2010)

[4] Majumdar S., "A review of magnetic resonance (MR) imaging of trabecular bone micro-architecture: contribution to the prediction of biomechanical properties and fracture prevalence," Technology Health Care 6(5-6): 321-7. (1998)

[5] Wassenaar, M. J. et. al., "High prevalence of vertebral fractures despite normal bone mineral density in patients with long-term controlled acromegaly," European Journal of Endocrinology, Volume 164, no.4, 475-83. (2011)

[6] Hans, D. et. al., "Correlations Between Trabecular Bone Score, Measured Using Anteroposterior Dual-Energy X-Ray Absorptiometry Acquisition, and 3-Dimensional Parameters of Bone Microarchitecture: An Experimental Study on Human Cadaver Vertebrae," Journal of Clinical Densitometry: Assessment of Skeletal Health, Volume 14, no.3, 302-312. (2011)

[7] Pothuand, L. and et al. "Correlations between grey-level variations in 2D projection images (TBS) and 3D microarchitecture: Applications in the study of human trabecular bone microarchitecture," Bone, Vol. 42, 775-787 (2008)

[8] Riggs B. L. et al, "Population-Based Study of Age and Sex Differences in Bone Volumetric Density, Size, Geometry, and Structure at Different Skeletal Sites," Journal of Bone and Mineral Research, Vol. 19, Issue 12. (2004)

[9] Johnell, O. and Kanis, J.A. "An estimate of the worldwide prevalence and disability associated with osteoporotic fractures," Osteoporos. Int. 17:1726. (2006).

[10] *Treatments To Prevent Fractures in Men and Women With Low Bone Density or Osteoporosis: An Update to the 2007 Report*, Comparative Effectiveness Review No. 53, prepared by the Southern California Evidence-based Practice Center, a Rand Health Center, under Contract No. HHSA 290-2007-10062-I for the Agency for Healthcare Research and Quality. (2012)

Publishing Agreement

It is the policy of the University to encourage the distribution of all theses, dissertations, and manuscripts. Copies of all UCSF theses, dissertations, and manuscripts will be routed to the library via the Graduate Division. The library will make all theses, dissertations, and manuscripts accessible to the public and will preserve these to the best of their abilities, in perpetuity.

Please sign the following statement:

I hereby grant permission to the Graduate Division of the University of California, San Francisco to release copies of my thesis, dissertation, or manuscript to the Campus Library to provide access and preservation, in whole or in part, in perpetuity.

Terry Lee

Author Signature

9/1/2015

Date